ChemComm

COMMUNICATION

View Article Online
View Journal | View Issue

Cite this: *Chem. Commun.*, 2023, 59, 11276

Received 12th August 2023,
Accepted 30th August 2023

DOI: 10.1039/d3cc03909a

rsc.li/chemcomm

Energetic performance of trinitromethyl nitrotriazole (TNMNT) and its energetic salts†

Sohan Lal [a] Richard J. Staples [b] and Jean'ne M. Shreeve *[a]

Little is known about trinitromethyl nitrotriazole (TNMNT) since the crystal structure, density, energetic performance, and thermal properties have not been determined. A detailed characterization of TNMNT and its hydrazinium and potassium salts and their potential as solid propellants and oxidizers has been established. TNMNT exhibits a high density (1.96 g cm^{-3}) and positive enthalpy of formation (ΔH_f = +84.79 kJ mol^{-1}). TNMNT and its hydrazinium and potassium salts illustrate excellent detonation properties (P = 34.24 to 36.22 GPa, D = 8899 to 9031 ms^{-1}). TNMNT and its hydrazinium salt exhibit outstanding propulsive properties (I_{sp} = 247.28 to 271.19 s), and these are superior to AP (I_{sp} = 156.63 s) and ADN (I_{sp} = 202.14 s). The results suggest opening the door to utilizing TNMNT and its energetic salts in solid rocket propulsion.

Finding a green alternative to ammonium perchlorate (AP) in solid rocket propulsion is highly demanded in the current era due to the many hazardous gaseous products (HCl, Cl_2, ClO, *etc.*) which are associated with AP, which are produced on its deflagration in the combustion process.[1] AP is an ideal oxidizer {oxygen balance (OB = 34%), (ρ = 1.95 g cm^{-3}), (T_d = 200 °C)}, which has triggered its use in AP-based composite propellants (with Al/GAP/HTPB) in space-related applications.[2] Very recently, various green-oxidizers have been developed, namely 3,4,5-trinitro-1-(trinitromethyl)-1*H*-pyrazole (**TNTNMP 1**),[3] 2,5-bis(trinitromethyl)-1,3,4-oxadiazole (**BTNMODA, 2**),[4] 3,5-dinitro-1-(trinitromethyl)-1*H*-pyrazol-4-amine (**TN-116, 3**),[5] 1,3-bis(trinitromethyl)-1*H*-1,2,4-triazole (**BTNMT, 4**)[6] and the unique (*Z*)-*N*,2,2,2-tetranitroacetimidic acid (**TNAA, 5**) (Fig. 1).[7]

Now in a series of new oxidizers for civil, space, and military applications, a novel energetic molecule, 3-nitro-1-(trinitromethyl)-1*H*-1,2,4-triazole (**TNMNT, 6**), and two of its energetic salts are described. The synthesis of compound **6** has been described previously but, its energetic performance and thermal characterization have not been reported.[8] Now for the first time, a detailed study on its modified, gram-scale synthesis and its energetic performance (potential oxidizer/fuel) with high-nitrogen energetic salts (**9–10**) was carried out and the results compared with top-performing explosives and oxidizers.

Commercially available 3-nitro-1*H*-1,2,4-triazole **7** was first reacted with chloroacetone to give **8** in excellent yield (95%). Compound **8** was reacted with mixed acid (100% HNO_3 and 98% H_2SO_4) at 0 °C to give **6**, which was reacted with different bases (NH_2NH_2 or KI) to form energetic high-nitrogen salts (**9–10**) (Scheme 1). Compounds **6–10** are solids at 25 °C. Their stabilities were measured with differential scanning calorimetry (DSC) and thermogravimetric analysis (TGA) at the two different heating rates of 5 °C and 10 °C min^{-1}.

Suitable crystals of compound **6** were obtained by the slow evaporation of methanol. It crystallizes in the monoclinic

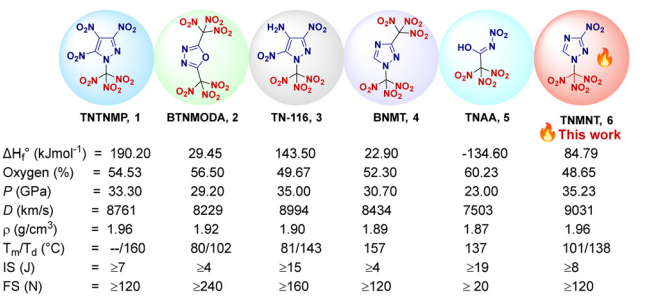

Fig. 1 Recently developed oxidizers and their unique properties.[3–6]

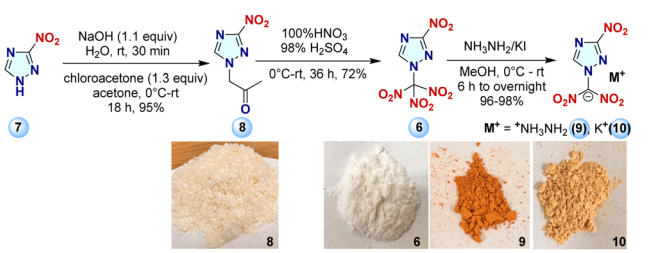

Scheme 1 Synthesis of **TNMNT** and its energetic salts.

[a] *Department of Chemistry, University of Idaho, Moscow, Idaho, 83844-2343, USA. E-mail: jshreeve@uidaho.edu; Fax: (+1)208-885-5173*

[b] *Department of Chemistry, Michigan State University, East Lansing, Michigan 48824, USA*

† Electronic supplementary information (ESI) available. CCDC 2253474 and 2255083. For ESI and crystallographic data in CIF or other electronic format see DOI: https://doi.org/10.1039/d3cc03909a

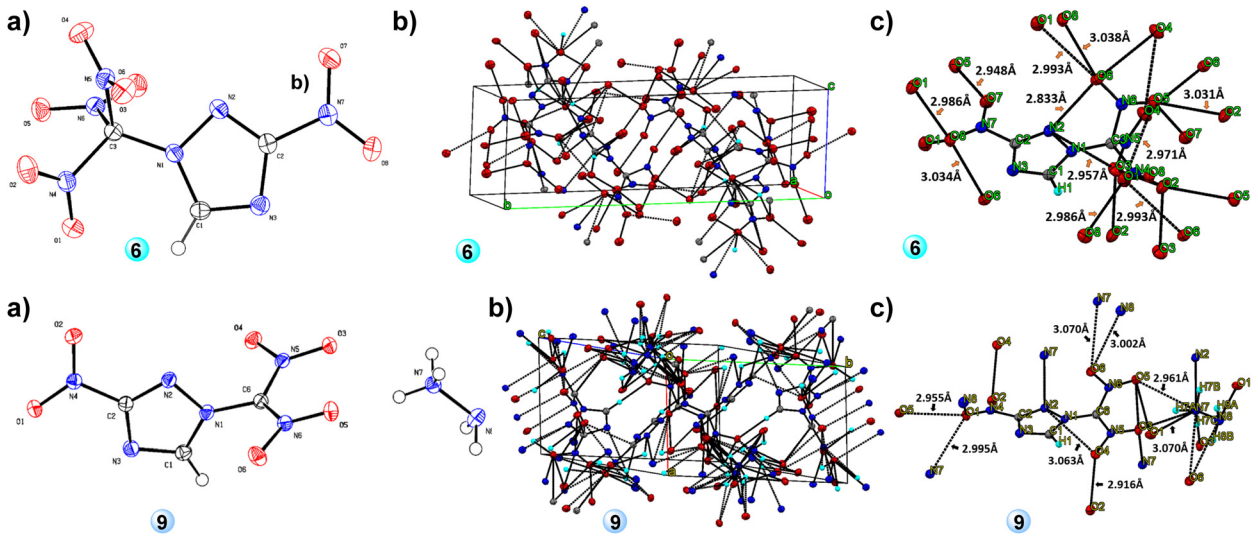

Fig. 2 (a) Single crystal X-ray structure (thermal ellipsoid plot (50%)), (b) packing diagram, and (c) H-bonds of **6** and **9**.

Table 1 Physicochemical properties of compounds **6** and **9–10**

Compound	**6**	**9**	**10·H$_2$O**	AP[a]	ADN[b]	RDX[c]
Formula[d]	$C_3HN_7O_8$	$C_3H_6N_8O_6$	$C_3HKN_6O_6$	NH_4ClO_4	$NH_4N(NO_2)_2$	$C_3H_6N_6O_6$
FW[e] [g mol^{-1}]	263.08	250.13	256.18	117.49	124.06	222.12
OB^{CO}[f] (%)	+27.37	0.0	−3.12	34.04	25.80	0.0
OB^{CO_2}[g] (%)	+9.12	−19.19	15.61	27.23	25.80	−21.61
N + O[h] [%]	85.92	83.18	70.28	66.39	96.75	81.06
O [%][i]	48.65	38.38	37.47	54.47	45	43.22
ΔH_f[j] [kJ mol^{-1}]	84.79	265.11	−12.44	−295.80	−149.72	70.30
ρ[k] [g cm^{-3}]	1.96	1.78	2.12	1.95	1.81	1.80
T_m/T_d[l] [°C]	101/138	137	225	200	159	205
D[m] [ms^{-1}]	9031	8952	8899	6368	7860	8867
P[n] [GPa]	35.23	34.24	36.22	15.80	23.60	34.07
IS[o] [J]	≥8	≥30	≥10	≥15	3-5	≥7.5
FS[p] [N]	≥120	≥240	≥80	≥360	64-72	≥120
I_{sp}[q] [s]	247.28	271.19	231.22	156.63	202.14	266.91
ρI_{sp}[r] [s]	484.67	482.72	490.19	306.15	365.87	480.45
I_{sp}[s] [s]	257.16	280.33	243.75	232.00	256.25	277.60
I_{sp}[t] [s]	266.13	258.09	235.90	262.11	272.91	259.56

[a] Ref.1, 2. [b] Ref. 2. [c] Ref. 2. [d] Molecular formula. [e] Molecular weight. [f] CO based oxygen balance. [g] CO_2 based oxygen balance. [h] N + O contents in %. [i] Oxygen content in %. [j] Calculated enthalpy of formation. [k] Measured densities, gas pycnometer at room temperature. [l] Melting point and decomposition temperature (onset) under nitrogen gas (DSC, 5 °C min^{-1}). [m] Calculated detonation velocity. [n] Calculated detonation pressure. [o] Measured impact sensitivity (IS). [p] Measured friction sensitivity (FS). [q] I_{sp} = specific impulse of neat compound (monopropellant). [r] ρI_{sp} = density specific impulse of neat compound (monopropellant). [s] I_{sp} = specific impulse at 88% compound and 12% Al. [t] I_{sp} = specific impulse at 78% compound, 12% Al (fuel additive) and 10% binder (HTPB). Specific impulse calculated at an isobaric pressure of 70 bar and initial temperature of 3300 K using EXPLO5 V 6.06.

space group *P*21/*c* and has a network of intermolecular H-bonds and π–π-interactions, contributing to the calculated high density of 1.999 g cm^{-3} at 100 K in good agreement with its measured density of 1.960 g cm^{-3} at 25 °C (see Fig. 2 and Tables S4–S8, ESI†). Compound **9** was crystallized by the slow evaporation of methanol in the monoclinic space group *P*21/c and has a good density of 1.809 g cm^{-3} (at 100 K) and 1.780 g cm^{-3} (at 25 °C), which are supported by the intermolecular H-bonds and π–π-interactions present in the molecule. The H-bonding interplay has a maximum 3.1 Å D–D distance and a minimum 110° angle present in **9**: N7–O1: 2.994 Å, N7–O2: 3.075 Å, N7–O3: 2.878 Å, N7–O3: 2.927 Å, N7–O4: 3.089 Å, N7–O5: 2.961 Å, N7–N2: 3.009 Å, N8–O1: 3.056 Å, N8–O6: 3.002 Å (see Fig. 2 and Tables S9–S13, ESI†).

Oxygen balance (OB, Ω), (the measurement of available oxygen after all hydrogens are converted to H_2O and all carbon atoms into CO or CO_2), plays an important role in the combustion process. **TNMNT** has a high positive OB^{CO} of +27.37%, comparable to the well-known oxidizer, ADN (OB^{CO} = +25.80%) and superior to RDX (OB^{CO} = 0.0%). It has a high density relative to AP (ρ = 1.95 g cm^{-3}), ADN (ρ = 1.81 g cm^{-3}), RDX (ρ = 1.80 g cm^{-3}) and HMX (ρ = 1.91 g cm^{-3}). Compound **10·H$_2$O** has the highest density (2.12 g cm^{-3}) in the series, which is superior to CL-20 (ρ = 2.04 g cm^{-3}).

The enthalpies of formation $(\Delta H_f^\circ(s))$ of the new compounds were calculated with the Gaussian 03 suite of programs[9] using the isodesmic method (see Fig. S1, ESI†). Corresponding propulsive and detonation properties were

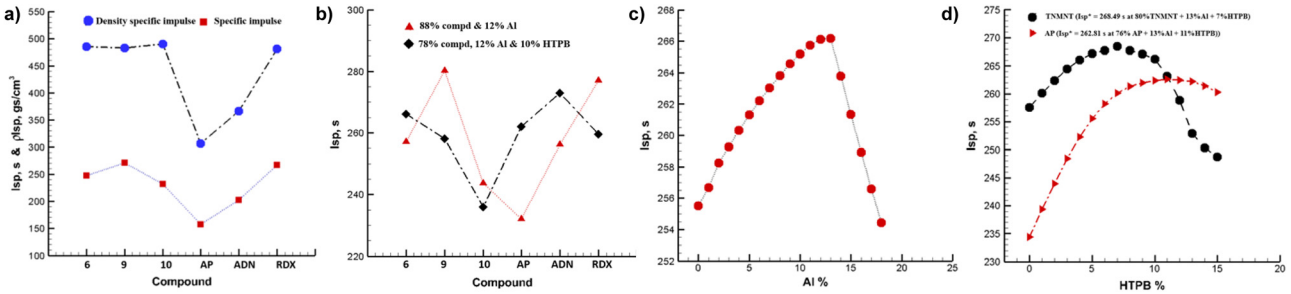

Fig. 3 (a) Comparison of propulsive properties (a) monopropellant (b) composite bipropellant. (c) **TNMNT** at 10% HTPB and varying the percentage of **TNMNT** (90–72%) and Al (0–18%). (d) **TNMNT** and AP at 13% Al and varying the percentage of **TNMNT**/AP (87–71%) and HTPB (0–16%).

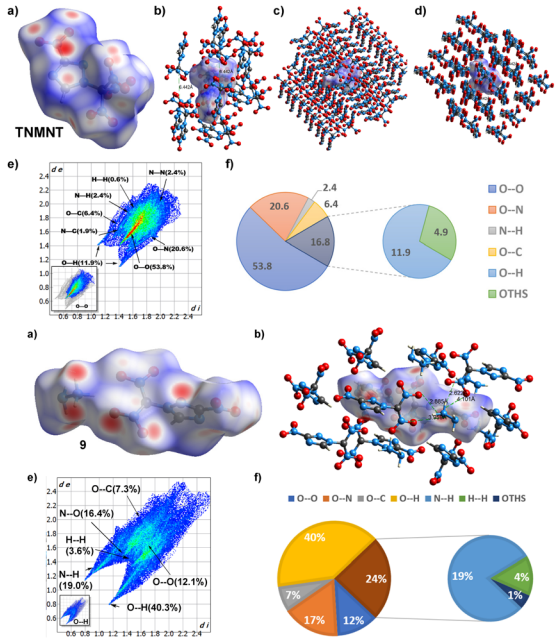

Fig. 4 (a) Hirshfeld surfaces. (b)–(d) close contacts. (e)–(f) Fingerprint plot and individual contacts.

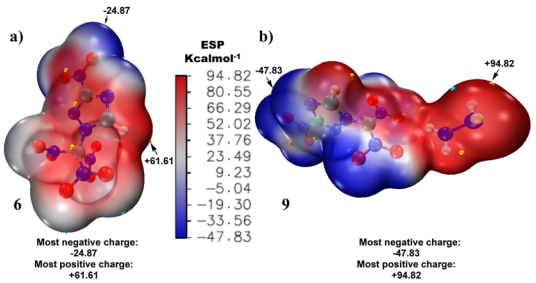

Fig. 5 (a) Electrostatic potential mapped compounds **6** and **9**, calculated at B3LYP/6-311++G(d,p) level.

estimated using $(\Delta H_f^\circ(s))$ and room temperature densities with the help of EXPLO5 V6.06 software.[10] Compounds **6** and **9** exhibit high positive enthalpies of formation $(\Delta H_f^\circ(s))$, 84.79 kJ mol^{-1} and 265.11 kJ mol^{-1}, respectively whereas compound **10·H$_2$O** has a negative $(\Delta H_f^\circ(s))$, −12.44 kJ mol^{-1}), as shown in Table 1. A comprehensive comparison of the

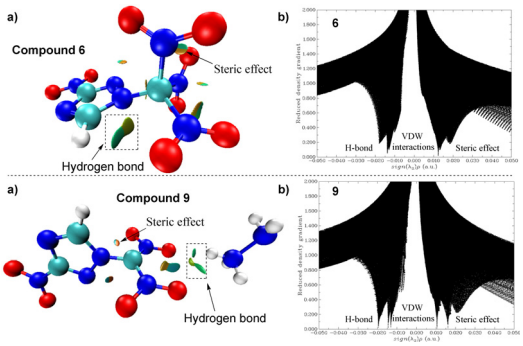

Fig. 6 Non-covalent interaction (NCI): (a) reduced density gradient (RDG) and (b) scatter diagram of compounds **6** and **9** at B3LYP/6-311++G(d,p) level.

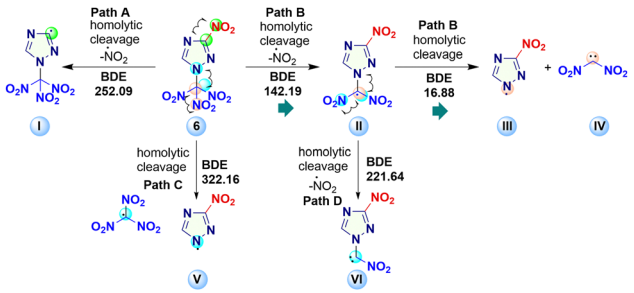

Fig. 7 Proposed thermal decomposition pathway for compound **6** (BDEs are given in kJ mol^{-1}).

propulsive properties of new materials reveal that compounds **6** and **9** show excellent potential as solid rocket fuels and compound **10** as a promising explosive, as shown in Fig. 3 and Table 1.

The physicochemical properties of materials are directly associated with their molecular structures. Hirshfeld surfaces. 2D-fingerprints were generated and visualized with CrystalExplorer 21.5 software,[11] which show that compounds **6** and **9** are rigidly packed and have several types of interactions within the crystal structure. In Hirshfeld surface analysis, red and blue dots on the compound surfaces illustrate high and low close contacts, respectively (Fig. 4a). Fingerprint plots suggest that H–O contacts for compounds **6** (∼11.9%), **9** (∼40.3%) and H–N contacts for compounds **6** (∼2.4%), and **9** (∼19.0%), contribute to the high stability of compound **9**. On the other hand, the high number of various close interactions such as N–O, N–N and O–O contacts in the

molecules, result in high impact sensitivity. This result is also supported by their measured impact sensitivities and the stability order is **RDX** < **6** < **9** (Table 1).

The electrostatic potential (ESP) map of **6** and **9** was predicted using B3LYP/6-311++G(d,p) level of theory and plotted with Multiwfn and VMD software.[12] The negative fraction (blue) and positive fraction (red) represent the more and less active spots on the molecular surface, respectively (Fig. 5). The hydrazinium cation of compound **9** is present under red surfaces, showing that it provides additional stability to the material. ESP minima and maxima for compounds **6** and **9**, are −24.87, −47.83 kcal mol^{-1} and +61.61, +94.82 kcal mol^{-1}, respectively.

The product of total variance and balance of charges ($\sigma_{tot}{}^2\upsilon$) for compounds **6** and **9** is 44.62 and 135.33, respectively and this is significantly higher than that of reference energetic materials such as RDX (27.29) and HMX (33.09). Whereas compound **9** exhibits the highest ratio of negative surface areas (61.20), resulting in comparatively high stability. The stability order is **RDX** < **HMX** < **6** < **9** (see Table S3, ESI†).

Compounds **6** and **9** have shown various interactions in their crystal structures, contributing to their high stability. Now, we have determined such types of non-covalent interactions and reduced density gradient using B3LYP/6-311++G(d,p) level of theory as illustrated in Fig. 6.

To better understand the decomposition process of **6**, the bond dissociation energy (BDE, gas-phase) of homolytic cleavage of various bonds was calculated using B3LYP/6-311++G(d,p) level of theory (Fig. 7). Results suggest that compound **6** is likely to decompose according to path B.

The detonation properties of compounds **6**, **9** and **10** were calculated using EXPLO5 V 6.06 program[10] using their $\left(\Delta H_f^\circ(s)\right)$ and experimental densities. The results are illustrated in Table 1. TNMNT and its energetic salts exhibit excellent detonation properties **6** (P = 35.23 GPa, D = 9031 ms^{-1}), **9** (P = 34.24 GPa, D = 8952 ms^{-1}) and **10**·$\mathbf{H_2O}$ (P = 36.22 GPa, D = 8899 ms^{-1}), which are comparable to RDX (D = 8867 ms^{-1}, P = 34.07 GPa). The mechanical stabilities of new compounds were determined by measuring their friction sensitivities (FS) and impact sensitivities (IS) using BAM friction tester and BAM drop hammer techniques[13] Compounds **6** and **9** have comparatively lower sensitivities (IS = 8 J, FS = 120 N for **6** and IS = 30 J, FS = 240 N for **9** to RDX ((IS = 7.5 J, FS = 120 N), which allow them to be stored at room temperature for a longer period and have great potential as a solid rocket propellant. Whereas, compound **10** was found slightly more sensitive to friction (IS = 10 J, FS = 80 N for **10**·$\mathbf{H_2O}$)

In summary, we have developed a straightforward synthesis route to TNMNT and its hydrazinium and potassium salts from commercially available 3-nitro-1*H*-1,2,4-triazole in excellent yields. Compounds **6–10** were fully characterized by various techniques such as FTIR, NMR, and elemental analyses. The structures of **6** and **9** were also further confirmed by single-crystal X-ray analysis. A detailed study on the energetic performance and thermal characterization of the new materials was also carried out. Compounds **6–10** possess moderate thermal stability (T_d, 137–225 °C) and low sensitivity to impact (8–30 J) and friction (120–240 N). Compound **6** melts (T_m = 101 °C) before decomposition (T_d, 138 °C) and exhibits excellent detonation properties (P = 35.23 GPa, D = 9031 ms^{-1}), which makes it a promising candidate as a melt castable green explosive. Compounds **9** (P = 34.24 GPa, D = 8952 ms^{-1}) and **10**·$\mathbf{H_2O}$ (P = 36.22 GPa, D = 8899 ms^{-1}) have excellent potential as solid propellants in rocket propulsion.

S. L. investigation, methodology, conceptualization and manuscript writing. R. J. S. X-ray data collection and structure solving. S. L. and J. M. S. conceptualization, manuscript writing-review and editing, supervision.

The Rigaku Synergy S Diffractometer was purchased with support from the National Science Foundation MRI program (1919565). We are grateful to the Fluorine-19 fund. The authors thank Prof. Haixiang Gao, for helpful discussions.

Conflicts of interest

The authors declare no competing financial interest.

Notes and references

1 (*a*) J. P. Agrawal, *High Energy Materials: Propellants, Explosives and Pyrotechnics*, Wiley-VCH, Weinheim, 1st edn, 2010; (*b*) H. Vogt, J. Balej, J. E. Bennett, P. Wintzer, S. A. Sheikh and P. Gallone, *Ullmann's Encyclopedia of Industrial Chemistry*, Wiley-VCH, 2002.
2 (*a*) F. P. Madyakin, *Components and combustion products of pyrotechnic compositions*, KGTU, Kazan, 2006, Vol. 1; (*b*) H. Gao and J. M. Shreeve, Azole-based energetic salts, *Chem. Rev.*, 2011, **111**, 7377–7436; (*c*) S. Lal, A. Chowdhury, N. Kumbhakarna, S. Nandagopal, A. Kumar and I. N. N. Namboothiri, Synthesis and energetic properties of homocubane based high energy density materials, *Org. Chem. Front.*, 2021, **8**, 531–548.
3 W. Zhang, Y. Yang, Y. Wang, T. Fei, Y. Wang, C. Sun and S. Pang, Challenging the limits of the oxygen balance of a pyrazole ring, *Chem. Eng. J.*, 2023, **451**, 138609.
4 Q. Yu, P. Yin, J. Zhang, C. He, G. H. Imler, D. A. Parrish and J. M. Shreeve, Pushing the limits of oxygen balance in 1,3,4-oxadiazoles, *J. Am. Chem. Soc.*, 2017, **139**, 8816–8819.
5 N. Ding, Q. Sun, X. Xu, Y. Li, C. Zhao, S. Li and S. Pang, Can a heavy trinitromethyl group always result in a higher density?, *Chem. Commun.*, 2023, **59**, 1939–1942.
6 G. Zhao, D. Kumar, P. Yin, C. He, G. H. Imler, D. A. Parrish and J. M. Shreeve, Construction of polynitro compounds as high-performance oxidizers via a two-step nitration of various functional groups, *Org. Lett.*, 2019, **21**, 1073–1077.
7 T. T. Vo, D. A. Parrish and J. M. Shreeve, Tetranitroacetimidic acid: A high oxygen oxidizer and potential replacement for ammonium perchlorate, *J. Am. Chem. Soc.*, 2014, **136**, 11934–11937.
8 (*a*) T. P. Kofman, G. Y. Kartseva, E. Y. Glazkova and K. N. Krasnov, *Russ. J. Org. Chem.*, 2005, **41**, 753–757; (*b*) T. P. Kofman, G. Y. Kartseva and E. Y. Glazkova, *Russ. J. Org. Chem.*, 2008, **44**, 870–873; (*c*) V. Thottempudi and J. M. Shreeve, *Synthesis*, 2012, **44**, 1253–1257.
9 M. J. Frisch, G. W. Trucks, H. B. Schlegel and G. E. Scuseria, *et al.*, *Revision D.01*, Gaussian Inc., Wallingford, CT, 2003.
10 M. Sućeska, EXPLO5, version 6.01, Brodarski Institute, Zagreb, Croatia, 2013.
11 P. R. Spackman, M. J. Turner, J. J. McKinnon, S. K. Wolff, D. J. Grimwood, D. Jayatilaka and M. A. Spackman, CrystalExplorer: A program for Hirshfeld surface analysis, visualization and quantitative analysis of molecular crystals, *J. Appl. Cryst.*, 2021, **54**, 1006–1011.
12 T. Lu and F. Chen, Multiwfn: A multifunctional wavefunction analyzer, *J. Comput. Chem.*, 2012, **33**, 580–592.
13 (*a*) Recommendations on the transport of dangerous goods, manual of tests and criteria, 7th revised edn, United Nations, New York 2019; (*b*) NATO, standardization agreement 4487 (STANAG4487), explosives, friction sensitivity tests 2002.